THE JOURNAL OF BIOLOGICAL CHEMISTRY
Vol. 279, No. 17, Issue of April 23, pp. 17301–17311, 2004

Printed in U.S.A.

Cholesterol-independent Interactions with CD47 Enhance $\alpha_v\beta_3$ Avidity*

Received for publication, November 21, 2003, and in revised form, February 6, 2004
Published, JBC Papers in Press, February 13, 2004, DOI 10.1074/jbc.M312782200

John F. McDonald, Alex Zheleznyak, and William A. Frazier‡

From the Department of Biochemistry and Molecular Biophysics, Washington University School of Medicine, St. Louis, Missouri 63110

Expression in OV10 cells of either wild-type CD47 or its extracellular IgV domain linked to a glycosylphosphatidylinositol anchor- (IgV-GPI) enhanced ligand-induced $\alpha_v\beta_3$ activation as detected by the binding of LIBS1 and LIBS6 mAbs. The amplitude of LIBS binding was greater with both CD47 and IgV-GPI expression, indicating an increase in the population of "activable" integrin molecules. Expression of either CD47 species also increased $\alpha_v\beta_3$-mediated adhesion to vitronectin, and to surfaces coated with the anti-β_3 antibody AP3, because of enhanced clustering of $\alpha_v\beta_3$ as confirmed by chemical cross-linking. Cholesterol depletion with methyl-β-cyclodextrin did not prevent the increase in anti-LIBS binding, but reduced cell adhesion to vitronectin and AP3. However, cells expressing CD47 were partially insulated against this disruption, and IgV-GPI was even more effective. Both CD47 and IgV-GPI were found in cholesterol-rich rafts prepared in the absence of detergent, but only CD47 could recruit $\alpha_v\beta_3$ and its associated signaling molecules to these domains. Thus CD47-$\alpha_v\beta_3$ complexes in cholesterol-rich raft domains appear to engage in G_i-dependent signaling whereas CD47-$\alpha_v\beta_3$ interactions that lead to integrin clustering are also detergent resistant, but are insensitive to cholesterol depletion and do not require the transmembrane region of CD47.

Integrins form complexes with other transmembrane proteins that can modulate their functions. Lateral integrin partners include growth factor receptors, tetraspanins, and CD47, an Ig family protein also known as integrin-associated protein (IAP) (1). CD47 is characterized by a single extracellular IgV domain, a 5-TM[1] region known as the multiple membrane-spanning (MMS) domain, and a short cytoplasmic tail that is alternatively spliced (2, 3). CD47 is both physically and functionally associated with β_3 and β_1 integrins (4, 5), and mediates a range of adhesion-related processes. Ligation of CD47 with thrombospondin (TSP), or a peptide, 4N1K, derived from its C-terminal domain, augments cell spreading and migration on $\alpha_v\beta_3$ substrates and $\alpha_{IIb}\beta_3$- and $\alpha_2\beta_1$-mediated platelet aggregation (6, 7). These actions are inhibited by pertussis toxin treatment, indicating a role for heterotrimeric G_i in CD47 signaling (8). In fact, detergent-stable complexes of CD47 and $G_i\alpha$ with both $\alpha_v\beta_3$ and $\alpha_{IIb}\beta_3$ have been isolated, suggesting that CD47 and the integrin may combine to form a functional 7-TM complex that functions like a G protein coupled receptor (4, 6, 8).

The $\alpha_v\beta_3$-CD47-G_i complex has also been found in Triton X-100-resistant membrane domains, or rafts, which are thought to act as organizing platforms for diverse signaling pathways, including those involving growth factors, G protein-coupled receptors, and T cell activation (9, 10). Depletion of membrane cholesterol was shown to destabilize the $\alpha_v\beta_3$-CD47-G_i complex in C32 melanoma and ovarian carcinoma cells, suggesting that intramembrane contacts controlling its localization to rafts may promote or even be required for complex assembly and G_i-coupled signaling (9). CD47-mediated signaling also occurs in Jurkat T cells, where treatment with certain anti-CD47 antibodies promotes apoptosis via a G_i-mediated pathway involving cyclic AMP regulation of cAMP-dependent kinase (11). Ligation of CD47 with other antibodies has been shown to have a synergistic effect on T cell activation that required the MMS domain of CD47 for both the T cell response and for raft localization (10). Thus raft localization may play a role in organizing CD47 signaling complexes in a number of systems.

Recently, effects of CD47 on β_3 integrin functions have been reported that appear to be independent of downstream signaling. $\alpha_{IIb}\beta_3$-mediated platelet aggregation was stimulated by TSP peptide in energy-depleted cells shown to be deficient in signaling (12). Furthermore, 4N1K peptide-induced activation of $\alpha_{IIb}\beta_3$, as measured by binding of PAC-1 antibody to transfected cells, required only the presence of the extracellular IgV domain of CD47, added either as a soluble protein or expressed with a generic membrane anchor (12). In addition, a previous study had shown that expression of the CD47 extracellular IgV domain in ovarian carcinoma cells was required for $\alpha_v\beta_3$-mediated binding of vitronectin-coated beads (13). These data indicate that the physical association of only the IgV domain of CD47 can affect β_3 integrin function. Thus CD47 may influence β_3 functions through interactions that involve different regions of the molecule. While it seems that signaling-dependent actions of CD47 may require cholesterol-rich domains, the possible role of membrane domains in more direct effects on the conformation of its associated integrin is unknown.

In this study, we have examined the ability of CD47 association to promote activated states of $\alpha_v\beta_3$, and addressed the role of detergent resistant membrane domains in CD47 modulation of integrin function. CD47 interactions with $\alpha_v\beta_3$ were found to promote both integrin activation induced by RGD peptide, and $\alpha_v\beta_3$ avidity in binding immobilized substrates by

* This work was supported by National Institutes of Health Grants HL54390 and GM57573 and National Institutes of Health Fellowship F32-HL10209 (to J. F. M.). The costs of publication of this article were defrayed in part by the payment of page charges. This article must therefore be hereby marked "*advertisement*" in accordance with 18 U.S.C. Section 1734 solely to indicate this fact.

‡ To whom correspondence should be addressed. Tel.: 314-362-3348; Fax: 314-362-7183; E-mail: frazier@biochem.wustl.edu.

[1] The abbreviations used are: TM, transmembrane; MMS, multiple membrane-spanning; mAb, monoclonal antibody; BSA, bovine serum albumin; FACS, fluorescent-activated cell sorting; CHAPS, 3-[(3-cholamidopropyl)dimethylammonio]-1-propanesulfonic acid; DRM, detergent-resistant micelles; CRD, cyclodextrin-resistant domains; GPI, glycosylphosphatidylinositol; LIBS, ligand-induced binding sites.

enhancing integrin clustering. These effects resulted from CD47-$\alpha_v\beta_3$ complexes that were resistant to cholesterol depletion, although they still resided in Triton-insoluble membrane domains. These CD47-$\alpha_v\beta_3$ complexes were distinct from those localized in cholesterol-rich domains, which were disrupted by cyclodextrin treatment, and required the MMS segment of CD47 for integrin and G protein association. Thus, both the physical nature of CD47-$\alpha_v\beta_3$ complexes and their effect on integrin functions can be influenced by their location in different membrane microdomains.

MATERIALS AND METHODS

Reagents and Cell Lines—The human ovarian carcinoma cells, known as OV10, were maintained as previously described (4). The stable transfections of $\alpha_v\beta_3$, CD47, and IgV-GPI have been previously reported by Lindberg *et al.* (13), and the cells used in this study were derived from the same lines. For all experiments, OV10 cells were previously treated with serum-free media for 16–18 h. Cell manipulations were carried out in Hanks Balanced Salt Solution containing 20 mM HEPES pH 7.5 (HBSS) with additional reagents for each application. Anti-β_3 mAbs AP3 (14) and 7G2 (15), and anti-CD47 2D3 and B6H12 (16) have been previously described. The anti-$\alpha_v\beta_3$ mAb LM609 and anti-$\alpha_v\beta_5$ mAbs P1F6 were generous gifts of Dr. David Cheresh (Scripps Research Institute), and the two ligand-induced binding sites (LIBS) antibodies, LIBS1 and LIBS6, were generously provided by Dr. Mark Ginsberg (Scripps Research Institute). Polyclonal antibodies for Western blots of integrin β_5 subunit, $G_i\alpha$, Gβ, Src, Lyn, and FAK were obtained from Santa Cruz Biotechnology, and the mAb for SHP-2 was purchased from Transduction Laboratories. FITC-anti-mouse IgG (Sigma Chemical Co.) was employed as the secondary antibody for flow cytometry experiments, and horseradish peroxidase conjugates of anti-rabbit IgG and anti-mouse IgG (Jackson Laboratories) were used for Western blots. The peptides 4N1K (KRFYVVMWKK), 4NGG (KRFYGGMWKK), and GRGDSP were synthesized as previously described (17). BCECF-AM was purchased from Molecular Probes, and BS^3 was from Pierce Chemical Co. Optiprep™ was obtained from Axis-Shield (Oslo, Norway). All other reagents were purchased from Sigma Chemical Company unless otherwise stated.

Cholesterol Depletion of OV10 Cells—5×10^6 cells were brought up at 1.25×10^6/ml in serum-free Iscoves media containing 0.1% fatty acid-free BSA with or without 10 mM methyl-β-cyclodextrin (Aldrich Chemicals) and incubated on a rocker at 37 °C for 20 min. This procedure has been shown to reduce total cellular cholesterol by 40% in OV10 cells (9). After washing, cells were resuspended in appropriate media or buffers for cell adhesion, lysis, or FACS staining.

Flow Cytometry—Expression of CD47, β_3, $\alpha_v\beta_3$, and LIBS epitopes in OV10 cells was measured by flow cytometry. 2×10^4 cells were resuspended in 50 μl of FACS buffer (1% BSA, 2 mM $MgCl_2$, 1 mM $CaCl_2$ in HBSS) with 10 μg/ml of primary antibody and incubated on ice for 30 min. For detection of LIBS binding, GRGDSP was included at 0.1–2 mM, and the incubation was carried out at 37 °C for 15 min followed by 15 min on ice. Cells were washed and incubated in 50 ml of the same buffer containing goat anti-mouse IgG-FITC (Fc-specific) at a 1:50 dilution for an additional 30 min. After washing, the cells were diluted to 0.4 ml and analyzed on a flow cytometer using the Cell Quest software program.

Cell Adhesion—A rapid, non-washing, fluorescence-based assay (18) was employed to measure cell adhesion at an early time point before cell spreading occurred. OV10 cells were resuspended at 1.25×10^6/ml in 5 ml of HBSS containing BCECF, and incubated on a rocker at 37 °C for 20 min. Cells were washed, resuspended in 4 ml of binding buffer (1.5% BSA, 2 mM $MgCl_2$, 1 mM $CaCl_2$ in HBSS) at 0.2×10^6/ml, and dispensed into V-well plate at 100 μl/well. The plate was incubated at 37 °C for 10 min, and immediately centrifuged at $1000 \times g$ for 10 min at 4 C. Unbound cells were detected from triplicate fluorescence measurements (fluorescein parameters) of cells at the bottom of wells as measured with an FLX800 plate reader (Bio-Tek Instruments, Inc.). Total cell fluorescence was determined from measurements of cells in uncoated wells. Percent cell binding was calculated based on the total cell fluorescence for each cell type and the unbound cell fluorescence for individual samples.

Isolation of Detergent-stable Complexes—Monoclonal antibodies AP3 and B6H12 were coupled to sheep anti-mouse 4.5-μm magnetic beads, and vitronectin was coupled to 4.5-μm tosyl-activated magnetic beads (Dynal) according to the manufacturer's protocols. 5×10^6 cells were resuspended in 1 ml of HBSS with 0.1 mM $MnCl_2$, and bound to substrate-coated magnetic beads (2×10^7) by mixing at room temperature for 20 min. Unbound cells were removed in the supernatant after placing the sample in a magnet, and the beads were washed 1× in the same way. Bead-bound cells were taken up in 1 ml of lysis buffer (HBSS containing 10 mM CHAPS, 250 mM sucrose, 0.1 mM $MnCl_2$, and protease inhibitor mixture), and mixed for 10 min at room temperature. Beads were resuspended in 20 μl of HBSS with 2.5 units of DNase I and incubated for 5 min at room temperature. Complexes were extracted with 2× sample buffer at 65 °C for 15 min and analyzed by SDS-PAGE and Western blotting.

Cross-linking of β_3 Aggregates—Cells were bound to AP3 or vitronectin-coated magnetic beads as described above. After washing, bead-bound cells were resuspended in 1 ml of HBSS containing 0.5–5 mM BS^3, and mixed at 4 °C for 90 min. The beads were resuspended in 1 ml of phosphate-buffered saline containing 0.1 M glycine and 1% BSA, and mixed at room temperature for 15 min. The isolated beads were then treated with lysis buffer and DNase I as described above, followed by analysis of β_3 integrin by SDS-PAGE and Western blotting.

Detergent-free Isolation of Rafts—The preparation was carried out according to the method of Smart *et al.* (19). Approximately 100×10^6 cells were resuspended in 1 ml of ice cold buffer A (20 mM Tris, pH 7.8, 0.25 M sucrose, 1 mM EDTA) and lysed with 20 strokes of a Dounce homogenizer, followed by extrusion through a 20-gauge needle 20×. The lysate was centrifuged at $1000 \times g$ for 10 min, and the supernatant was collected. The pellet was subjected to the same homogenization procedure just described, and the supernatants were combined and brought up to 2 ml with buffer A. The sample was layered over 8 ml of 30% Percoll in buffer A, and centrifuged in a 75 Ti rotor on a Beckman L8-80 M Ultracentrifuge at $84{,}000 \times g$. The plasma membrane fractions normally migrated near the middle of the gradient as detected by Western blotting for transferrin receptor (not shown), and could be visually distinguished as a discrete band. This region was collected by pipette and brought up to 2 ml with buffer A. To this sample was added 1.84 ml of buffer C (50% Optiprep in 120 mM Tris, pH 7.8, 0.25 M sucrose, 6 mM EDTA) + 0.164 ml buffer A, over which was layered an 8-ml Optiprep gradient of 10–20% (made from dilutions of buffer C in buffer A). The sample was centrifuged in an SW41 rotor at $52{,}000 \times g$ for 90 min. The top 5 ml containing the light membranes were collected and mixed with 4 ml of buffer C. The lower 4 ml were pooled and taken as the raft-depleted membranes. The light membrane mixture was placed in an ultracentrifuge tube, over, which was layered 3 ml of a 4% Optiprep solution (made by diluting buffer C with buffer A). The sample was centrifuged in the SW41 rotor as before to produce a membrane band clearly visualized at the gradient interface. This material was collected by pipette and taken as the purified raft fraction.

Separation of Triton-soluble from Triton-insoluble Cell Fractions—This procedure was similar to the method described by Maile *et al.* (20), and is based on the association of detergent-resistant domains with the cytoskeletal pellet (21). 5×10^6 cells were lysed in 1 ml of ice-cold lysis buffer (0.2% Triton X-100 in HBSS containing 2 mM $MgCl_2$, 1 mM $CaCl_2$, and protease inhibitor mixture) and clarified by centrifugation at $14{,}000 \times g$ for 10 min at 4 °C. The supernatant was collected and taken as the Triton-soluble fraction. The pellet was resuspended at room temperature in 1 ml of HBSS containing 1% Nonidet P-40, 0.25% sodium deoxycholate, 2 mM $MgCl_2$, 1 mM $CaCl_2$, and protease inhibitors, followed by centrifugation as before. This supernatant was collected and taken to be the Triton-insoluble fraction, with the remaining pellet containing the insoluble cytoskeleton. SDS-PAGE and Western blotting were carried out on 50-μl aliquots of the Triton-soluble and Triton-insoluble fractions for each condition.

RESULTS

Binding of LIBS Antibodies to $\alpha_v\beta_3$ Is Enhanced by CD47 Expression—To determine if CD47 expression can have a direct influence on $\alpha_v\beta_3$ activation, binding of antibodies recognizing LIBS was measured for OV10 cells co-transfected with CD47 and β_3 integrin. The transfection and selection of clones for the cell lines employed in this study have been previously reported (13). Transfection of these cells with only β_3 chain results in expression of $\alpha_v\beta_3$ as a result of assembly with endogenous α_v. This does not result in overexpression because the level of $\alpha_v\beta_3$ expression is limited by the level of α_v and is near the level of $\alpha_v\beta_5$ expressed in wild-type OV10 cells (9). CD47 was expressed in these cells in its wild-type form and as a fusion protein containing the IgV domain linked to a glycophosphatidylinositol anchor (IgV-GPI) (13). As compared with wild-type CD47,

the IgV-GPI species has been shown to be deficient in downstream T cell signaling induced by CD47 ligation (22) (10). On the other hand, as discussed above, IgV-GPI supported vitronectin-coated bead binding when co-expressed with $\alpha v\beta 3$, and so may serve as an indicator of signaling-independent effects of CD47 (13). As measured by flow cytometry (Fig. 1, *A* and *B*), expression levels of wild-type CD47 and IgV-GPI were within 5% of each other, and levels of $\alpha_v\beta_3$ were also comparable among the cell lines employed, with a general order of IgV-GPI > CD47-> CD47+ (Fig. 1*B*). To correct for the small differences in integrin expression, anti-LIBS mAb binding was normalized to the binding of non-LIBS antibody LM609. Based on the LIBS1/LM609 binding ratio, neither wild-type CD47 nor IgV-GPI activated $\alpha_v\beta_3$ in the absence of RGD or Mn^{2+} (not shown). However, RGD-induced binding of LIBS-1 was enhanced with expression of either CD47 species (Fig. 1, *A* and *C*), with IgV-GPI producing the largest effect. Binding of LIBS6 was also increased with CD47 expression, and again IgV-GPI produced a larger increase in the maximal level of RGD-induced binding compared with wild-type CD47 (Fig. 1*D*). The enhanced binding appeared to result from an increase in the maximal binding at saturating RGD concentrations (Fig. 1*E*). Thus surface expression of the IgV domain of CD47 resulted in an increase in the number of "activable" integrin molecules, or the fraction of $\alpha_v\beta_3$ susceptible to stimulation by RGD peptide. The thrombospondin C-terminal peptide 4N1K was also tested for an ability to induce LIBS binding, but at concentrations up to 100 μM, no effect was observed either in the presence or absence of RGD for any cell line (not shown). Because cholesterol has been shown to be a component of the CD47-integrin complex (9), the effects of cholesterol depletion on activation of LIBS epitopes was examined. Rather than reducing anti-LIBS binding to CD47-expressing cells, cholesterol treatment had only small effects on binding of LIBS1 or LIBS6 for any of the cell lines, and differences in relative levels of anti-LIBS binding with CD47 or IgV-GPI expression was unchanged by cyclodextrin treatment (Fig. 1, *C* and *D*). Thus membrane cholesterol depletion did not disrupt the CD47-mediated changes in $\alpha_v\beta_3$ that are responsible for anti-LIBS binding. That IgV-GPI induced a larger change in binding of LIBS antibodies than wild-type CD47 may indicate that transmembrane contacts might even constrain the ability of the extracellular domain of CD47 to induce conformational changes in $\alpha_v\beta_3$. In any case, the stimulation of RGD-induced binding of LIBS1 and LIBS6 indicated that IgV-integrin interactions promoted a conformational change in $\alpha_v\beta_3$ that is associated with its activation.

CD47 Enhances $\alpha_v\beta_3$-mediated Adhesion through Cyclodextrin-resistant Effects—To evaluate the effects of CD47 on $\alpha_v\beta_3$-mediated cell adhesion, a rapid binding assay was used to measure OV10 cell attachment to V-well plates coated with vitronectin at high (5 μg/ml) and low (1 μg/ml) densities. At the high density, a high percentage of cells (65–80%) were bound irrespective of CD47 expression, and for all cell lines, treatment with RGD peptide reduced the binding to low levels (3–7%). Thus the assay was specific for RGD-containing substrates. Because the OV10 cells can bind to vitronectin through both $\alpha_v\beta_3$- and $\alpha_v\beta_5$-mediated adhesion, the $\alpha_v\beta_5$-blocking antibody P1F6 (4) was employed to determine $\alpha_v\beta_3$-specific effects. Cell attachment at the high ligand density showed no effect of either wild-type CD47 or IgV-GPI expression, and no major reduction was observed in cells treated with P1F6 (Fig. 2*A*). Thus, at this level of vitronectin, $\alpha_v\beta_3$-mediated adhesion supported nearly maximal cell attachment that was not reliant on CD47 expression. However, with cyclodextrin treatment, binding of CD47-deficient cells was reduced to about 20%, but cells expressing wild-type CD47 or IgV-GPI bound at levels of about 40 and 60%, respectively (Fig. 2*A*). While it is not known precisely how cholesterol depletion disrupted cell adhesion, alteration of the membrane environment could in theory influence either the ligand binding conformation of both $\alpha_v\beta_3$ and $\alpha_v\beta_5$, or the clustering of integrin molecules, as has been reported for $\alpha_5\beta_1$ and LFA-1 (23). However, expression of either CD47 or IgV-GPI partially protected against this effect (Fig. 2*A*). Co-treatment with P1F6 and cyclodextrin did not further reduce the binding of the cells compared with cyclodextrin alone (Fig. 2*A*), indicating that $\alpha_v\beta_3$-mediated adhesion predominated in the cholesterol-depleted cells, and the influence of CD47 was exerted on that integrin. Treatment with LM609 to block $\alpha_v\beta_3$-mediated adhesion did not reduce cell binding (Fig. 2*A*), indicating that $\alpha_v\beta_5$ alone also supported adhesion at a high vitronectin density. However, blocking $\alpha_v\beta_3$ in cyclodextrin-treated cells reduced binding to a low level irrespective of CD47 expression (Fig. 2*A*), indicating that $\alpha_v\beta_5$-mediated adhesion was not rescued from the disruptive effects of cholesterol depletion. Thus expression of either wild-type CD47 or IgV-GPI protected the cells against the disruption of cell binding caused by cholesterol depletion by enhancing $\alpha_v\beta_3$-mediated adhesion, but not adhesion conferred by $\alpha_v\beta_5$.

At the low ligand density, cell binding was reduced to about one-fourth of the high vitronectin density level for all three cell lines, and was blocked in all cases with RGD peptide (Fig. 2*B*). Whereas no effect of wild-type CD47 or IgV-GPI expression was detected in untreated cells, with P1F6 treatment, cell binding to vitronectin was reduced to a low level in CD47-deficient cells (Fig. 2*B*). Thus, at low substrate conditions, $\alpha_v\beta_3$-mediated binding was not supported, and $\alpha_v\beta_5$-mediated adhesion predominated. However, for cells expressing wild-type CD47 or IgV-GPI, only moderate or no reduction of binding was observed with P1F6 treatment (Fig. 2*B*), indicating that when $\alpha_v\beta_5$-mediated binding was blocked at low substrate conditions, the remaining $\alpha_v\beta_3$-mediated adhesion was CD47-dependent. For cyclodextrin-treated cells at the low vitronectin density, binding of CD47-deficient cells was reduced to a low level, and wild-type CD47 conferred only minor protection (Fig. 2*B*). However, binding of IgV-GPI-expressing cells was resistant to cholesterol depletion, and co-treatment with P1F6 and cyclodextrin did not result in a further significant disruption of cell adhesion (Fig. 2*B*), indicating the residual adhesion was because of$\alpha_v\beta_3$. Thus IgV-GPI exhibited an even greater protective effect against the cyclodextrin-induced disruption of cell binding than wild-type CD47. Blocking $\alpha_v\beta_3$-mediated binding with LM609 treatment reduced binding to a lower level in all the cell lines. However, this amount of $\alpha_v\beta_5$-mediated binding was eliminated with cholesterol depletion with no effect of CD47 expression (Fig. 2*B*), indicating that a CD47-independent effect of cholesterol depletion on $\alpha_v\beta_5$-mediated binding was displayed at the low ligand density.

In summary, expression of either wild-type CD47 or IgV-GPI was shown to enhance $\alpha_v\beta_3$-mediated adhesion, as detected both by an increase in binding of cells at low ligand density (Fig. 2*B*) and by protection against cyclodextrin-induced disruption of cell binding conferred at both high and low substrate conditions (Fig. 2*A*).

CD47 Enhances $\alpha_v\beta_3$ Avidity for Binding Immobilized Substrate—The effect of CD47 or IgV-GPI expression to increase the fraction of integrins activated upon treatment with saturating RGD peptide (Fig. 1*E*) suggests that their interactions with $\alpha_v\beta_3$ can shift the integrin conformational equilibrium toward the activated state. However, enhanced cell adhesion could also be derived from an increase in avidity because of changes in the aggregation state of $\alpha_v\beta_3$ that result in cell-matrix contacts with a higher valency. To determine if expres-

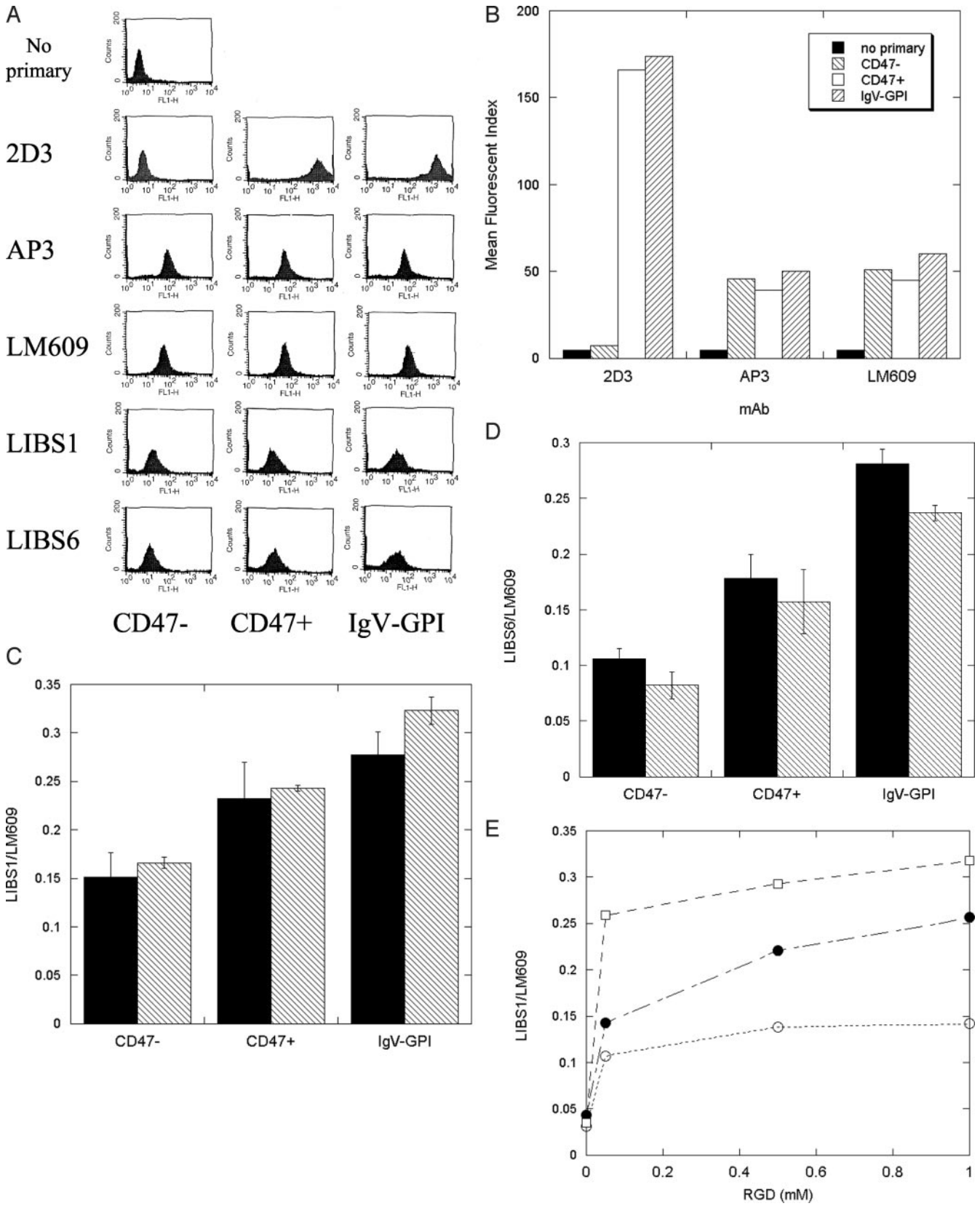

FIG. 1. **RGD-induced appearance of LIBS epitopes is increased with CD47 expression.** Protein expression was measured by flow cytometry for OV10 cells expressing $\alpha_v\beta_3$ alone (*CD47*−), $\alpha_v\beta_3$ and wild-type CD47 (*CD47*+), or $\alpha_v\beta_3$ and IgV-GPI. For detection of LIBS epitopes, cells were incubated with LIBS1 or LIBS6 antibodies in the presence of 2 mM GRGDSP peptide for 15 min at 37 °C and 15 min on ice, followed by normal washing and secondary antibody treatments. *A*, flow cytometry profiles. Primary antibodies are listed in the *left column* for detection of CD47 (*2D3*), β_3 (*AP3*), $\alpha_v\beta_3$ (*LM609*), and ligand-induced binding sites in β_3 (LIBS1, LIBS6). *B*, relative expression levels of CD47, β, and $\alpha_v\beta_3$ for the three cell types: CD47−, *right-hatch*; CD47+, *open*; IgV-GPI, *left-hatch*. *C*, binding of LIBS1 normalized to binding of LM609 for the three cell types: *filled*, untreated; *right-hatch*, cyclodextrin-treated. *D*, binding of LIBS6 normalized to binding of LM609 for the three cell types: *filled*, untreated; *right-hatch*, cyclodextrin-treated. *E*, concentration curve for LIBS1 binding induced by treatment with millimolar concentrations of GRGDSP under the same conditions as described above. CD47−, *open circles*; CD47+, *filled circles*; IgV-GPI, *open squares*.

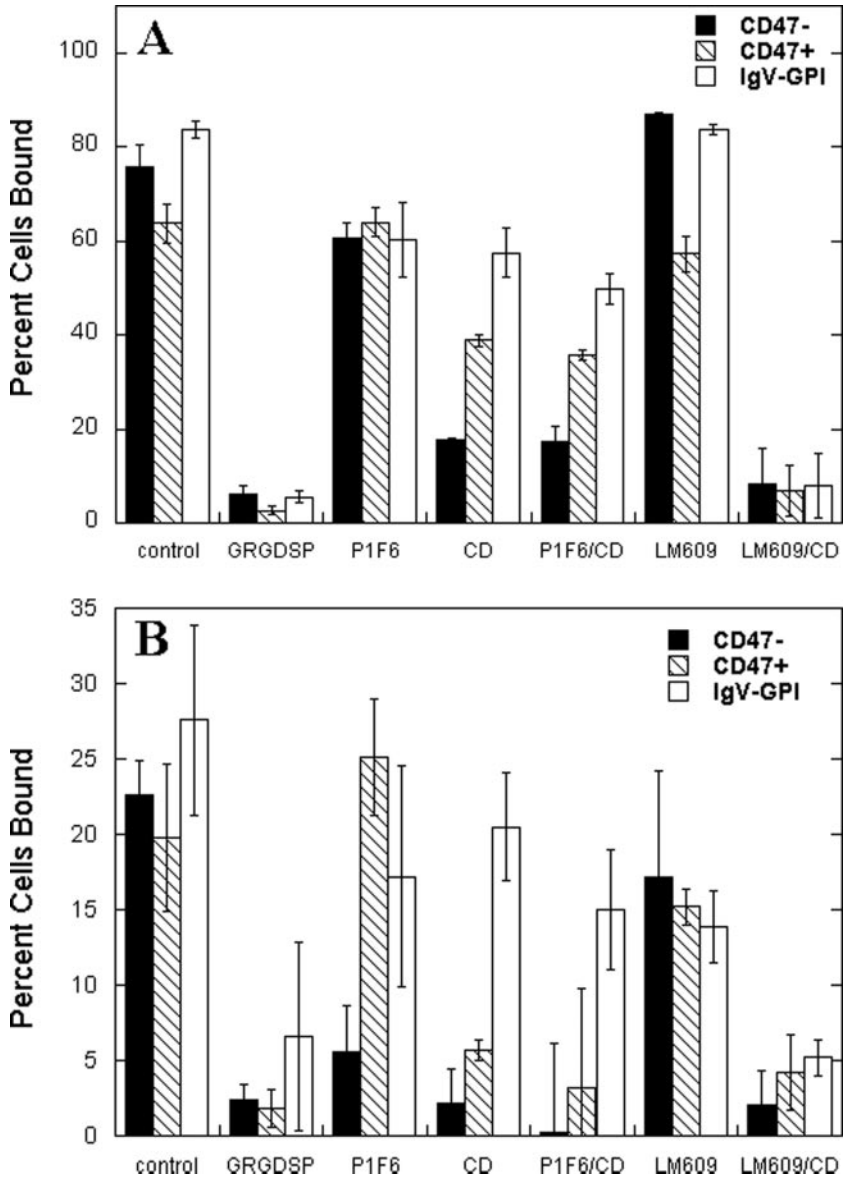

FIG. 2. **CD47 enhances $\alpha_v\beta_3$-mediated binding to vitronectin.** OV10 cells were resuspended at 1.25×10^6/ml in HBSS containing BCECF and incubated on a rocker for 20 min at 37 °C prior to application into vitronectin-coated wells. For experiments evaluating the effects of cholesterol depletion, the dye-loaded cells were resuspended at 1.25×10^6/ml in HBSS containing 0.1% fatty acid-free BSA with and without 10 mM methyl-β-cyclodextrin, and incubated on a rocker for 20 min at 37 °C before binding. Treatment with antibodies or peptide was carried out immediately prior to application in binding buffer at 1.25×10^6/ml, and incubated at 37 °C for 15 min followed by direct dilution to the final binding suspension. *A*, binding of ovarian carcinoma cells to vitronectin coated at high density (5 μg/ml). *B*, binding of cells to vitronectin coated at low density (1 μg/ml). CD47−, *filled*; CD47+, *right-hatch*; IgV-GPI, *open*. X-axis labels indicate treatment with 1 mM GRGDSP peptide (GRGDSP), 20 μg/ml of anti-$\alpha_v\beta_5$ antibody (P1F6), 50 mg/ml of anti-$\alpha_v\beta_3$ antibody (LM609), 10 mM methyl-β-cyclodextrin (*CD*), or a combination of antibody, and methyl-β-cyclodextrin (P1F6/CD, LM609/CD).

sion of CD47 enhances $\alpha_v\beta_3$ avidity, cell attachment to plates coated at high and low densities of anti-β_3 antibody AP3 was measured. AP3 ligation of integrin molecules should occur at a constant antibody-antigen affinity, thus any difference in cell binding must be derived from an increase in $\alpha_v\beta_3$ avidity. At the higher AP3 density, no significant differences in cell adhesion were observed among the three cell types, with each displaying the same maximal level of binding. At the lower antibody density, binding of CD47-deficient cells was reduced by 80%, but binding of cells expressing wild-type CD47 expression was reduced by only about 20%, and IgV-GPI-expressing cells bound to the low density of AP3 to the same extent as on high density AP3 (Fig. 3*A*). Thus, expression of either wild-type CD47 or IgV-GPI increased the binding of $\alpha_v\beta_3$ to immobilized AP3 antibody, presumably by increasing the valency of cell surface contacts by enhancing integrin clusters. As with vitronectin binding, the effects of CD47 became superfluous at higher ligand densities (Fig. 2*A*).

We next examined the effects of cholesterol depletion on $\alpha_v\beta_3$ avidity. Membrane cholesterol levels have been reported to affect the clustering of $\alpha_5\beta_1$ in rat fibroblasts (23), and in T-cells, via the GPI-anchored protein CD24 (24). Because we have shown that anti-LIBS binding is not significantly affected by cyclodextrin treatment (Fig. 1, *C* and *D*), its ability to disrupt cell adhesion to vitronectin (Fig. 2, *A* and *B*) may have been based in part on an inhibition of integrin clustering. At the high AP3 density, we observed a dramatic decrease in binding of CD47-deficient cells, consistent with a disruption of integrin clustering (Fig. 3*A*). However, nearly twice the level of binding was observed for wild-type CD47-expressing cells as for deficient ones, and IgV-GPI expression provided nearly complete protection against the cyclodextrin-induced disruption (Fig. 3*A*). Thus, as was also observed for vitronectin binding, expression of IgV-GPI gave an even greater enhancement of AP3 binding than wild-type CD47, and was more resistant to cholesterol depletion (Fig. 3*A*). For cell binding to AP3 at a low coating concentration, cholesterol depletion was completely disruptive in all the cell types, suggesting that CD47 expression could not compensate for the decreased valency resulting from both the reduced clustering induced by cyclodextrin and the low substrate density. We conclude from these experiments that interactions of the extracellular domain of CD47 with $\alpha_v\beta_3$ enhance binding of the integrin to immobilized substrates by promoting a greater degree of clustering to increase integrin avidity.

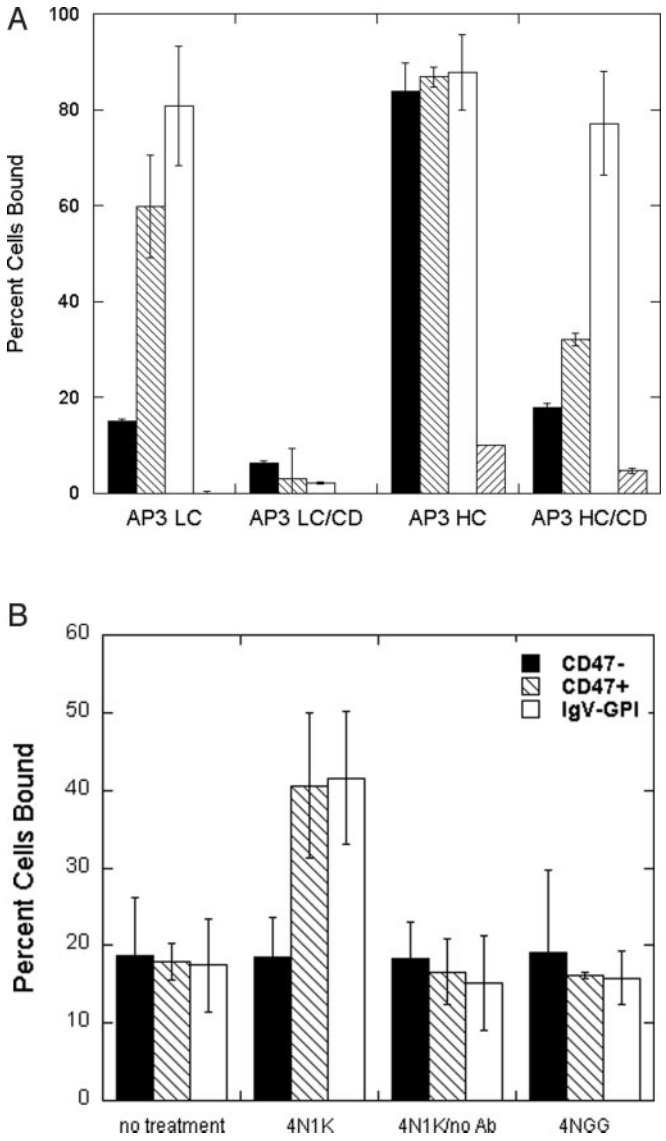

FIG. 3. **CD47 enhances $\alpha_v\beta_3$ avidity in binding surface coated anti-β_3 antibody.** OV10 cells were loaded with BCECF on a rocker for 20 min at 37 °C, and resuspended in binding buffer prior to application into antibody-coated wells. 4N1K treatment was carried out immediately before application in binding buffer at 1.25×10^6/ml, and incubated at 37 °C for 15 min followed by direct dilution to the final binding solution. *A*, binding of ovarian carcinoma cells expressing $\alpha_v\beta_3$ alone (*filled*), $\alpha_v\beta_3$ and wild-type CD47 (*right-hatch*), or $\alpha_v\beta_3$ and IgV-GPI (*open*) to AP3 coated at low density (LC, 10 μg/ml) and high density (HC, 50 μg/ml). *B*, treatment of 4N1K induces binding of $\alpha_v\beta_3$ to surface-coated antibody. X-axis indicates cells bound to surface coated with 2 μg/ml AP3. Cells were either left untreated, treated with 50 μM 4N1K, treated with 50 μM 4NGG, or treated with 50 μM 4N1K on an uncoated surface, as indicated by X-axis labels.

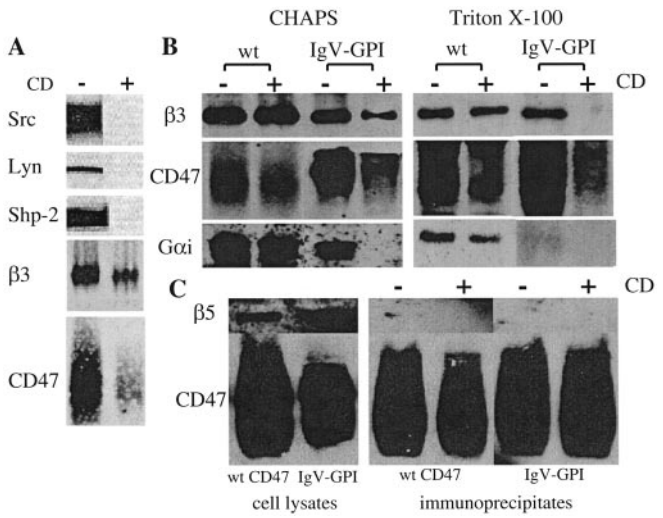

FIG. 4. **Cyclodextrin sensitivity of CD47-$\alpha_v\beta_3$ complexes.** *A*, β_3 immunoprecipitates adsorbed to AP3-coated magnetic beads from CHAPS lysates of cells expressing $\alpha_v\beta_3$ and wild-type CD47 were blotted for proteins indicated in *left column*. *B*, CD47 immunoprecipitates adsorbed to B6H12-coated magnetic beads from CHAPS or Triton X-100 lysates of cells expressing $\alpha_v\beta_3$ and either wild-type CD47 (*wt*) or IgV-GPI were blotted for β_3 and CD47. *C*, CD47 immunoprecipitates adsorbed to B6H12-coated magnetic beads from CHAPS lysates of cells expressing $\alpha_v\beta_3$ and either wild-type CD47 or IgV-GPI were blotted for β_5 and CD47. Untreated (−) and treated (+) with 10 mM methyl-β-cyclodextrin (*CD*).

4N1K Treatment Promotes IgV-$\alpha_v\beta_3$ Interactions That Enhance Integrin Avidity—Recently, the thrombospondin C-terminal peptide 4N1K was reported to induce $\alpha_{IIb}\beta_3$-mediated activation in signaling-deficient cells via CD47 (12), suggesting that the peptide may interact with CD47 to produce signaling-dependent and -independent effects on β_3 integrins. Furthermore, a recent report has shown that treatment with a similar peptide can increase $\alpha_v\beta_3$-mediated adhesion (25). However, we saw no effect of 4N1K on the binding of LIBS antibodies to OV-10 cells expressing either wild-type or IgV-GPI, either alone or with GRGDSP treatment (not shown), indicating that the peptide did not influence RGD-induced activation. We therefore tested the ability of 4N1K to enhance $\alpha_v\beta_3$ avidity by measuring OV-10 cell binding to AP3-coated plates, at coating concentrations that supported only nonspecific attachment by untreated cells. Although 4N1K has been reported to have CD47-independent effects on integrin functions in some situations (25, 26), no increased binding with peptide treatment was observed for CD47-deficient cells (Fig. 3*B*). However, enhanced binding was indeed observed with 50 μM 4N1K treatment of OV-10 cells expressing wild-type CD47 and IgV-GPI (Fig. 3*B*). Treatment with the control peptide 4NGG did not promote increased binding, and 4N1K treatment did not affect cell binding to uncoated, blocked wells (Fig. 3*B*). Thus, 4N1K peptide association with CD47 must stabilize a conformation of the IgV domain that interacts with $\alpha_v\beta_3$ to promote integrin clustering. Cyclodextrin treatment resulted in reduced background binding to less than 5%, as well as blocking the 4N1K effect (not shown), suggesting that its disruptive effects on avidity could not be overcome with peptide treatment.

CD47 Forms Cyclodextrin-resistant Complexes with $\alpha_v\beta_3$ through Its Extracellular Domain—Previous studies have reported a CD47-$\alpha_v\beta_3$ complex that is sensitive to cholesterol depletion (9), but the effects on integrin avidity that we report are not. We used immunoadsorption assays in detergent lysates with and without cyclodextrin treatment to distinguish direct association from co-localization in cholesterol-rich rafts. Cells expressing wild-type CD47 were allowed to bind magnetic beads coated with anti-β_3 mAb AP3 and lysed in CHAPS. Complexes were rapidly isolated and analyzed for signaling molecules associated with rafts (27). Indeed, Src, Lyn, SHP-2, and G_i were detected in association with the $\alpha v\beta 3$ complexes (Fig. 4*A*). Prior cyclodextrin treatment virtually eliminated all of these associations, an indication of the loss of integrity of CHAPS-resistant rafts (Fig. 4*A*). The level of wild-type CD47 was also reduced, indicating that a significant fraction of the CD47 was released with loss of raft integrity, and was thus likely to be indirectly associated with the integrin. Adsorption of complexes with anti-CD47-coated beads more clearly demonstrated β_3 association that was cyclodextrin-resistant in either CHAPS (Fig. 4*B*, *left panel*) or Triton X-100 (Fig. 4*B*, *right*

panel). Thus $\alpha_v\beta_3$ appeared to reside in several membrane compartments, with some associated with CD47 in cyclodextrin-sensitive rafts, some associated in cyclodextrin-resistant complexes, and some unassociated with CD47. Adsorption of IgV-GPI displayed cyclodextrin-resistant β_3 association in CHAPS lysates (Fig. 4*B*), indicating that the extracellular domain of CD47 was sufficient to bind $\alpha_v\beta_3$. In contrast, although integrin β_5 subunit and both forms of CD47 were clearly detected in cell lysates, β_5 was barely detected in CHAPS immunoprecipitates adsorbed with either wild-type CD47 or IgV-GPI, and no trace at all was observed with cholesterol depletion (Fig. 4*C*). These observations are consistent with the previous report that $\alpha_v\beta_5$ is present but not enriched in cholesterol-rich rafts, and the lack of association of this integrin with CD47 (9) (13). IgV-GPI adsorption from Triton X-100 lysates was greatly reduced upon cholesterol depletion, and β_3 was not detected (Fig. 4*B*, *right panel*), indicating that the stability of the complex in this detergent displayed a cholesterol dependence that was not observed in CHAPS solutions. However, detection of $G_i\alpha$ with wild-type CD47 was largely resistant to cyclodextrin treatment in complexes isolated with either detergent (Fig. 4*B*, *left panel*), indicating its association was not strictly based on raft integrity and was probably direct. On the other hand, $G_i\alpha$ was only found with IgV-GPI in CHAPS lysates, and its detection was completely cyclodextrin-sensitive (Fig. 4*B*, *left panel*), indicating that the MMS region is required for G protein association. In summary, analysis of immunoadsorbed complexes showed CD47 association with $\alpha_v\beta_3$ that was cyclodextrin-resistant and required only the IgV domain, in contrast to raft-localized signaling molecules and G proteins.

CD47 Promotes Formation of High Molecular Weight β_3 Species That Can Be Chemically Cross-linked—CD47-dependent effects on avidity are presumed to influence clustering of $\alpha_v\beta_3$ and should result in closer integrin-integrin contacts upon oligomerization. To detect oligomeric $\alpha_v\beta_3$, chemical cross-linking of cells with adsorbed anti-β_3 coated magnetic beads was employed, using the membrane-impermeable reagent BS^3. Detection of cross-linked species by this method requires close proximity of surface-exposed lysines on associated proteins, which also must be in a favorable orientation. Treatment with BS^3 before bead binding resulted in detection of only monomeric β_3 (Fig. 5*A*, *lanes 1* and *4*), indicating that cross-linked species were not formed in the absence of antibody engagement. Furthermore, this particular reagent did not cross-link the α_v and β_3 subunits under these conditions. However, upon BS^3 treatment following bead binding to the cells, but before cell lysis, higher order β_3-containing species were detected by Western immunoblotting of the bead-bound material (Fig. 5*A*). At least three types of complexes with a molecular weight greater than monomeric β_3 were detected. For CD47-deficient cells, an ~300 kDa species was detected at a significant level, and was further enriched with a higher concentration of BS^3 (Fig. 5*A*, *lanes 2* and *3*). Trace amounts of an approximately ~200 kDa species and a very high molecular weight band that barely migrated were also detected, and the larger species were not increased at the higher concentration of cross-linker (Fig. 5*A*, *lanes 2* and *3*). In contrast, for CD47-expressing cells, the ~300 kDa species was absent, but instead, very high molecular weight species were detected at significant levels even at the lower concentration of cross-linker (Fig. 5*A*, *lane 5*). These species were further enriched at the higher concentration, and only then did the ~300 kDa species appear (Fig. 5*A*, *lane 6*). Thus CD47 expression promoted the formation of the highest molecular weight β_3-containing aggregates. We also used beads coated with vitronectin, a natural ligand of $\alpha_v\beta_3$. Once again, the very high molecular weight species were present only in CD47-containing complexes (Fig. 5*A*, *lanes 9* and *10*). However, the ~300 kDa species was absent in both cell types (Fig. 5*A*, *lanes 7–10*) suggesting that it might be a complex of β_3 with the AP3 antibody. Treatment of cells with cross-linker before binding of cells to vitronectin-coated beads also did not produce higher molecular weight species (not shown). Thus, formation of the very large integrin aggregates required the presence of CD47. CD47 itself was only detected in monomeric form when treated with the same conditions (not shown), indicating it may not be accessible to direct covalent linkage with integrin. While the detection of cross-linked species indicates a protein-protein interaction, lack of detection does not rule it out, and could be because of poor orientation of lysines for cross-linking, destruction of the antibody epitope by BS^3, or lack of reagent accessibility to the protein-protein contacts. Cross-linked complexes from IgV-GPI-expressing cells adsorbed to anti-β_3 antibody AP3 were similar to those of wild-type CD47, with formation of the very high molecular weight β_3 species and no detection of the ~300 kDa species (Fig. 5*B*). Thus, formation of the large β_3 aggregates was mediated by the extracellular IgV domain of CD47 alone. Cyclodextrin treatment inhibited formation of cross-linked complexes in CD47-expressing cells, however, with IgV-GPI expression, cholesterol depletion resulted in complexes that were not significantly different compared with untreated cells (Fig. 5*B*). Thus, as suggested in the cell adhesion assays, promotion of β_3 aggregates by IgV-GPI was more resistant to cholesterol depletion than were aggregates formed by CD47.

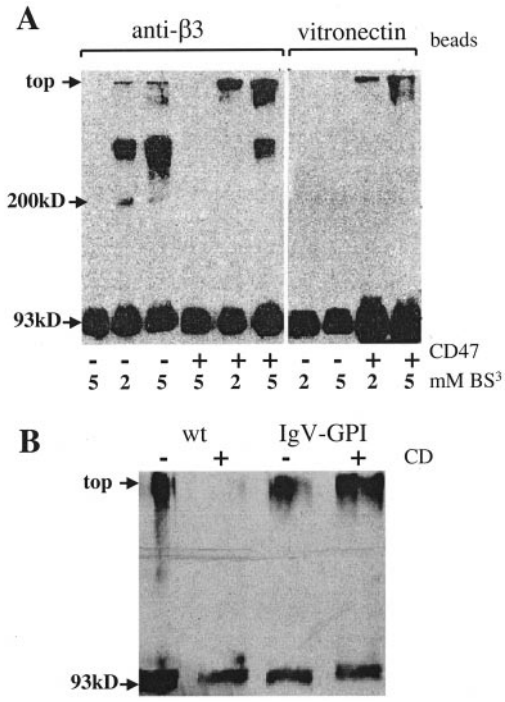

FIG. 5. **Detection of cross-linked aggregates of β_3 with CD47 expression.** Ovarian carcinoma cells were adsorbed to antibody- or vitronectin-coated magnetic beads as previously described. Bead-bound cells were treated with BS^3 for 90 min while rotated at 4 °C, quenched in 0.1 M glycine and 1% BSA, lysed, and analyzed by SDS-PAGE and Western blotting for β_3 integrin. *A*, detection of high molecular weight β_3 aggregates with wild-type CD47 expression. Magnetic beads were coated with AP3 or vitronectin, bound to ovarian carcinoma cells expressing $\alpha_v\beta_3$ alone (−) or with wild-type CD47 (+), and treated with BS^3 at indicated millimolar concentrations. *B*, cyclodextrin (*CD*) sensitivity of β_3 aggregate formation. AP3-coated magnetic beads were bound to cells previously treated with 10 mM methyl-β-cyclodextrin (+) or left untreated (−), followed by reaction with 2 mM BS^3, as described under "Materials and Methods." After detergent lysis, β_3 species were detected by SDS-PAGE and Western blotting.

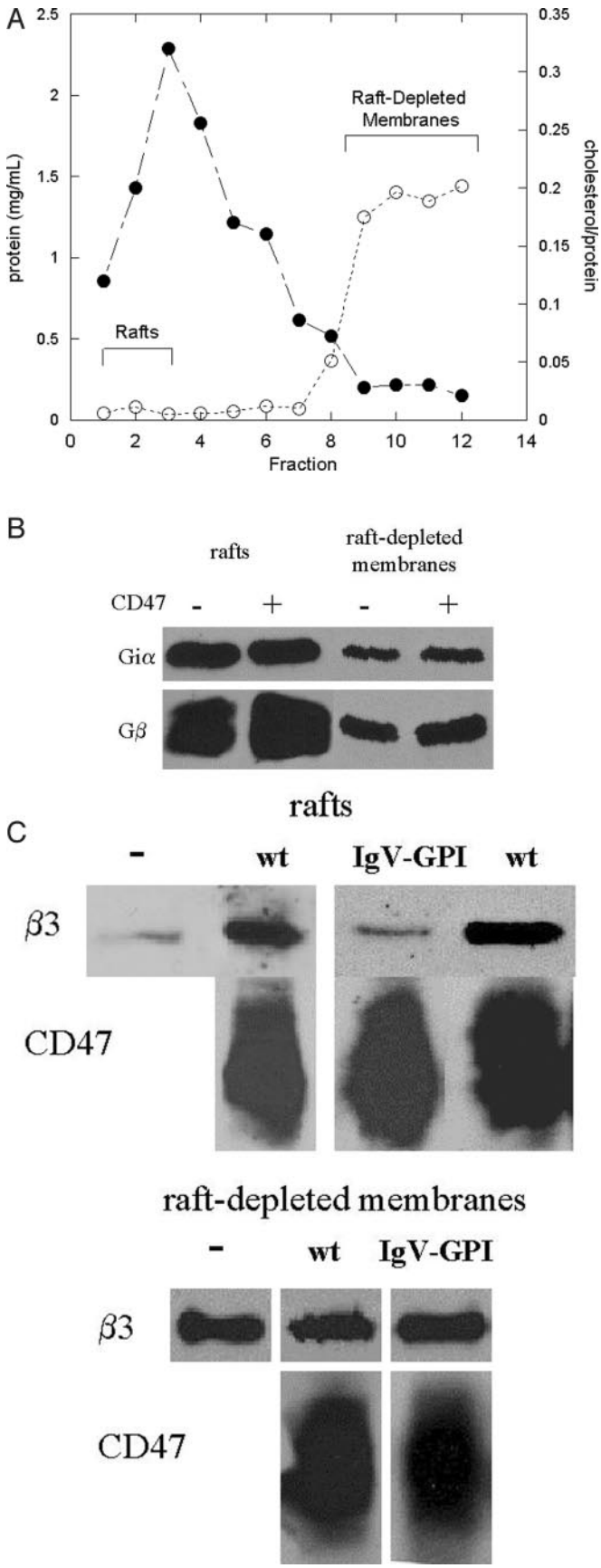

FIG. 6. **Detergent-free isolation of rafts from ovarian carcinoma cells.** Approximately 100×10^6 cells were resuspended in 1 ml of buffer A (see "Materials and Methods"), lysed with a dounce homogenizer and needle extrusion, and centrifuged at $1000 \times g$ for 10 min to collect the supernatant. The process was repeated with the pellet, and the combined supernatants were layered over 30% Percoll and centrifuged at $84,000 \times g$ to separate plasma membrane, which was collected near the middle of the gradient. The purified plasma membranes were adjusted to 46% sucrose in 4 ml over which was poured an 8 ml of 10–20% Optiprep gradient. The sample was centrifuged at $52,000 \times g$ for 90 min to separate cholesterol-rich rafts, which were collected in the top 5 ml, from the raft-depleted fractions in the lower 4 ml. The raft fractions were concentrated by mixing with 4 ml of 50% Optiprep solution, over which was layered 3 ml of a 4% Optiprep solution. The sample was centrifuged at $52,000 \times g$ for 90 min to produce a membrane band that was clearly visualized at the gradient interface, and collected by pipette as the purified raft fraction. Rafts were isolated for cells expressing $\alpha_v\beta_3$ alone (CD47−), $\alpha_v\beta_3$, and wild-type CD47 (CD47+), or $\alpha_v\beta_3$ and IgV-GPI (IgV-GPI). Proteins were detected by SDS-PAGE and Western blots for equal amount of protein loaded (20 μg). *A*, separation of cholesterol-rich rafts from raft-depleted membranes. Optiprep gradient fractions were analyzed for protein (mg/ml, left axis, *filled circles*) and cholesterol/protein (mass ratio, right axis, *open circles*). *B*, Western blots of $G_i\alpha$ and $G\beta$ in cholesterol-rich rafts *versus* raft-depleted membranes. *C*, Western blots of β_3 and CD47 in cholesterol-rich rafts (*left panel*) *versus* raft-depleted membranes (*right panel*) for cells expressing $\alpha_v\beta_3$ alone (−), $\alpha_v\beta_3$, and wild-type CD47 (*wt*), or $\alpha_v\beta_3$ and IgV-GPI (IgV-GPI).

MMS Region of CD47 Is Required for Targeting $\alpha_v\beta_3$ to Cholesterol-rich Rafts—To determine the dependence on CD47 of αvβ3 localization to cholesterol-rich membrane microdomains, we utilized detergent-free membrane preparations (19). This method has been used to isolate ordered lipid domains that display the greatest cholesterol enrichment, and are free of detergent-related artifacts (28). Purified plasma membranes were fractionated on Optiprep™ gradients, resulting in a small protein peak floating near the top (rafts) that separated from the major protein peak near the bottom (raft-depleted membranes), with a difference in the cholesterol/protein ratio of about 10-fold (Fig. 6*A*). These rafts are cholesterol-rich, and are distinguished from the more general "detergent-resistant domains" (DRMs). The large majority of the total plasma membrane protein resided in the lower half of the gradient, with the light fractions representing about 2% of the protein loaded (Fig. 6*A*). Cyclodextrin treatment resulted in elimination of the rafts, while not altering recovery of the bulk plasma membrane fractions (not shown). Western blots revealed that, for equal amounts of protein, the raft fraction was enriched in $G_i\alpha$ and $G\beta$ (Fig. 6*B*), consistent with the known targeting of these molecules to ordered domains by lipid modifications. Wild-type CD47 and IgV-GPI were found in both raft and raft-depleted membrane fractions (Fig. 6*C*), and levels of β_3 were the same in raft-depleted membranes from all three cell lines (Fig. 6*C*, *right*). However, upon analysis of equal amounts of protein from isolated rafts, β_3 was present in significant amounts only when the rafts were derived from cells expressing wild-type CD47 (Fig. 6*C*, *left*). Expression of IgV-GPI did not result in a β_3/CD47 ratio in rafts that was significantly different from CD47-deficient cells (Fig. 6*C*). Thus IgV-integrin interactions alone were not sufficient for targeting integrin to cholesterol-rich domains, indicating that transmembrane or cytoplasmic contacts in the wild-type CD47-$\alpha_v\beta_3$ complex are required for the integrin to partition into the light membranes. Because localization of CD47-$\alpha_v\beta_3$ complexes in these domains has been found to be required for the G protein-coupled cell spreading stimulated by thrombospondin-based agonists (9), this finding supports the model in which integrin association is required for downstream signaling (8). In T cells, IgV-GPI was not able to support downstream effects that included increases in $[Ca^{2+}]_i$, actin polymerization and PKCθ association with the cytoskeleton, that were correlated with synergistic activation with the TCR induced by CD47 ligation (22) (10). Thus, the MMS domain appears to be required for CD47 signaling in both of these systems. However, it is clear that IgV-GPI does in fact associate with $\alpha_v\beta_3$ (Fig. 4*B*) and alters its avidity (Fig. 3, *A* and *B*),

although this must occur in heavy membrane fractions, which are *not* rich in membrane cholesterol (Fig. 6*A*). This conclusion is consistent with the observation that, as noted above, the heavy membrane region of the gradient contained both wild-type CD47 and IgV-GPI in the same relative enrichment as the raft fractions, as well as the majority of the $\alpha_v\beta_3$ (Fig. 6*C*). Thus, interactions of the IgV domain of CD47 with $\alpha_v\beta_3$ that influence integrin activation and avidity do not require localization to cholesterol-rich rafts, in contrast to downstream signaling which also requires the MMS region of CD47.

CD47 and IgV-GPI Associate with $\alpha_v\beta_3$ in Cyclodextrin-resistant Membrane Domains—While IgV-GPI interactions with $\alpha v\beta 3$ could *not* take place in cholesterol-rich rafts (Fig. 6*C*), their localization in other types of DRMs may mediate the effects of CD47 on integrin function. It is becoming increasingly clear that membrane microdomains are heterogeneous (29). Recent studies have found that raft isolation based on detergent insolubility produces a more heterogeneous mixture of membrane domains than detergent-free preparations (30). In fact, detection of CD47 in light fractions from gradients of detergent lysates has been shown to be unaltered by cyclodextrin treatment (9), and other studies have reported the existence of similar cyclodextrin-resistant domains (31) (32). Recently, it was demonstrated that CD47 can move out of rafts by following its partitioning between Triton-soluble cell extracts and Triton-insoluble fractions that are associated with low speed cytoskeletal pellets (20). Using this method, we found both CD47 and IgV-GPI exclusively in the Triton-insoluble pellets, indicating they resided in DRMs associated with the cytoskeleton (Fig. 7*A*, *lanes 9* and *11*). Thus, this pellet fraction must include the cholesterol-rich rafts that were detected in detergent-free preparations (Fig. 6*A*). Cyclodextrin treatment resulted in the release of more than half of the wild-type CD47 in a Triton-soluble form (Fig. 7*A*, *lane 4 versus lane 10*), presumably as a result of disruption of cholesterol-rich rafts. IgV-GPI, on the other hand, persisted in the pellet and was not detected in the soluble extract even after cyclodextrin treatment (Fig. 7*A*, *lanes 6* and *12*). Complexes of $\alpha_v\beta_3$ with IgV-GPI were therefore localized in cyclodextrin-resistant domains (CRDs), while wild-type CD47-$\alpha_v\beta_3$ complexes were distributed in *both* CRDs and cholesterol-rich rafts. In all three cell lines, β_3 integrin was mostly Triton-soluble (Fig. 7*A*, *upper panel*), and this soluble fraction was increased with cyclodextrin treatment (*lanes 2*, *4*, and *6*), indicating that Triton extraction of $\alpha_v\beta_3$ from ordered lipid domains was increased with cholesterol depletion. However, the release of integrin with cyclodextrin treatment was increased when either CD47 or IgV-GPI was present (Fig. 7*A*, *lanes 4*, *6*, and *9–12*). Thus, CD47 enhanced partitioning of $\alpha_v\beta_3$ into detergent-resistant domains though IgV interactions that did not require the MMS region.

To demonstrate that CD47 associates with $\alpha_v\beta_3$ in the cyclodextrin-resistant domains, protein complexes were adsorbed to anti-CD47 coated beads from octylglucoside extracts of the Triton-insoluble pellets. These immunoprecipitation conditions were similar to those used in the previous study reporting an association of the IgV domain of CD47 with $\alpha_v\beta_3$ (13). Western analysis revealed the presence of β_3 upon adsorption of either wild-type CD47 or IgV-GPI from the Triton-insoluble, but octylglucoside-soluble fractions (Fig. 7*B*). Furthermore, detection of β_3 was not blocked by cyclodextrin treatment for either species (Fig. 7*B*), indicating that the CD47-$\alpha_v\beta_3$ interaction was stable upon cholesterol depletion. Thus, CD47 associates with $\alpha_v\beta_3$ in cyclodextrin-resistant domains via IgV interactions, which led to enrichment of the integrin in those membrane compartments.

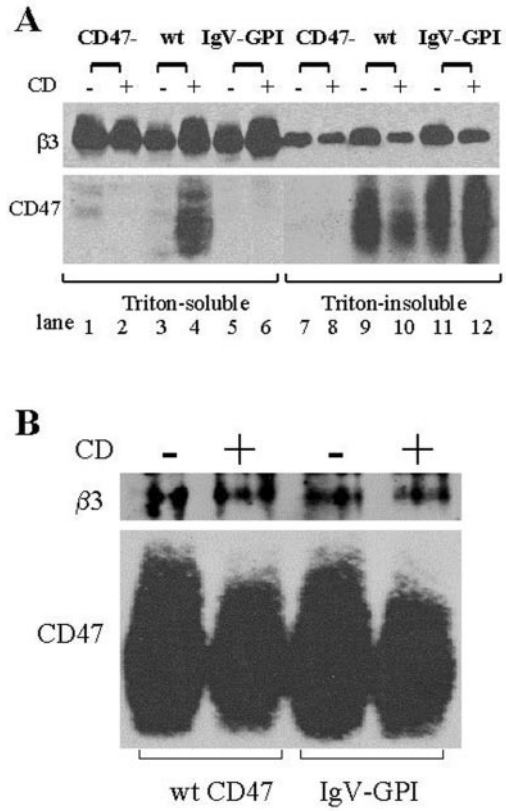

FIG. 7. **$\alpha_v\beta_3$ and CD47 associate in cyclodextrin-resistant membrane domains.** *A*, partitioning of $\alpha_v\beta_3$ and CD47 into Triton-soluble and Triton-insoluble fractions. OV10 cells expressing $\alpha_v\beta_3$ alone (−), $\alpha_v\beta_3$ and wild-type CD47 (+), or $\alpha_v\beta_3$ and IgV-GPI (*G*) were left untreated (−) or treated with 10 mM methyl-β-cyclodextrin (+) before extraction with Triton X-100. 5×10^6 cells per sample were extracted with 1 ml of 0.2% Triton X-100 by continuous rocking on ice for 1 h, followed by centrifugation to obtain a supernatant taken as the Triton-soluble fraction. Triton-insoluble pellets were brought up in the same volume of 1% Nonidet P-40, 0.25% sodium deoxycholate, 0.1% SDS and treated in the same way, but at room temperature, to obtain a supernatant taken as the triton-insoluble fraction. Equal volumes (100 μl) were analyzed by SDS-PAGE and Western blotting for β_3 and CD47. *B*, $\alpha_v\beta_3$ and CD47 association in Triton-insoluble fraction. OV10 cells were treated as above to yield Triton-insoluble pellets, which were extracted with 1% octylglucoside for 1 h at 4 C. The clarified extract was mixed with anti-CD47 antibody (B6H12) and anti-mIgG magnetic beads (50 μl) for an additional 1 h at 4 °C. The beads were washed once in the same buffer and analyzed by SDS-PAGE and Western blotting for β_3 (7G2) and CD47 (B6H12).

DISCUSSION

CD47 can modulate integrin function in two ways. The first of these is analogous to the well described activation of integrins such as $\alpha_{IIb}\beta_3$ on platelets by G protein-coupled receptors like the thrombin receptor (33). This so called inside-out signaling leads to activation of kinase pathways that modify integrins or their associated proteins, which in turn promotes a more active, perhaps higher affinity, state of the integrin (33). In addition to this classical signaling pathway, accumulating evidence indicates that direct interactions between CD47 and the integrins, which it modulates play a role. Importantly, ligation of CD47 by TSP-derived agonist peptides such as 4N1K and 7N3 (VVM motif peptides) seems to promote both pathways of integrin activation. We and others (4, 25, 34) have reported that these agonist peptides act via a G_i-dependent signaling pathway to augment integrin functions. In addition, there have been reports that the agonist peptides can augment integrin function even when G_i is inactivated by pertussis toxin, suggesting that there may be G protein-independent

routes of action (3). In fact a recent report showed that the soluble, extracellular IgV domain of CD47, when added to cells, could activate $\alpha_{IIb}\beta_3$ (12). This occurred only when the agonist peptide 4N1K was present, suggesting that 4N1K induces a conformation of the CD47 IgV domain that interacts favorably with the extracellular domain of $\alpha_{IIb}\beta_3$.

In this study we used the panel of OV-10 cells expressing the integrin $\alpha_v\beta_3$ alone, along with wild-type CD47 or with the extracellular IgV domain of CD47 engineered to be expressed anchored to the cell surface via GPI (13). This CD47 variant allowed us to study the signaling (G_i) independent actions of CD47 while maintaining the IgV domain in its normal location on the cell surface. The levels of CD47 and IgV-GPI expression in the OV10 cells in this study are in line with levels seen for natively expressed CD47 in a number of cell types, and does not represent overexpression. Likewise, the $\alpha_v\beta_3$ utilizes the endogenously expressed pool of α_v and is equivalent to the level of $\alpha_v\beta_5$ in wild-type cells. Given the earlier report of a role for cholesterol in stabilizing the CD47-integrin-G_i complex (9), we investigated the effect of cholesterol chelation on the ability of these two forms of CD47 to impact $\alpha_v\beta_3$ function. To our surprise, the GPI anchored CD47 IgV domain was as active as wild-type CD47 in promoting $\alpha_v\beta_3$-mediated adhesion and conformational changes associated with LIBS mAb binding, and was even more effective than native CD47 in protecting against the disruption of cell adhesion associated with the removal of cholesterol and dissolution of cholesterol-rich raft domains. The mechanism of these effects appears to be promotion of integrin clustering by CD47 and this clustering is not solely dependent on cholesterol-rich domains. Nonetheless, the inclusion of the integrin in cholesterol-rich light membranes along with associated Gi and other signaling proteins occurs only when native CD47 containing the MMS domain is expressed. Wild-type CD47 clearly exists in cholesterol-rich rafts as well as in other types of membrane domains. Thus it appears that CD47 residence in different membrane domains may alter its functions in terms of how integrin modulation is accomplished, and in the nature of that modulation

The mechanism by which CD47 promotes $\alpha_v\beta_3$ clustering is not known, but its interactions presumably stabilize an integrin conformation that is able to form integrin-integrin contacts. Recent studies of $\alpha_{IIb}\beta_3$ have shown that homo-oligomerization of β_3 can drive integrin clustering via transmembrane contacts, and that mutations which promote oligomerization also increase binding to fibrinogen (35). Similarly, we show that CD47 interactions promote both clustering of $\alpha_v\beta_3$ and increased activation as measured by binding of LIBS antibodies. Furthermore, models of integrin activation indicate that it is accompanied by separation of the α- and β-chains (36), suggesting that homo-oligomerization involves activated conformations, and drives a conformational equilibrium toward the activated state. That CD47 expression enhances the binding of anti-LIBS antibodies (Fig. 1, *A–E*) also indicates that it influences an activated integrin state. These events may be mediated by recruitment of $\alpha_v\beta_3$ to detergent-resistant domains (DRMs). A comparison of the effects of cholesterol depletion on the ability of wild-type CD47 *versus* IgV-GPI to alter $\alpha_v\beta_3$ avidity and raft localization supports such a mechanism. While wild-type CD47 expression conferred partial resistance to cyclodextrin-induced disruption of cell adhesion to $\alpha_v\beta_3$ ligands, IgV-GPI-expressing cells exhibited almost complete protection (Figs. 2 and 3). This was correlated with the partial conversion of wild-type CD47 to a Triton-soluble state with cholesterol depletion, while IgV-GPI localization in Triton-insoluble domains was completely resistant to cyclodextrin treatment (Fig. 7). Thus, IgV-GPI appeared to be superior to wild-type CD47 in its ability to confer protection against cyclodextrin-induced disruption of cell adhesion as a result of its increased enrichment in cyclodextrin-resistant membrane domains. A correlation between raft localization and integrin clustering has been previously reported in fibroblasts, where membrane cholesterol levels affected the clustering of $\alpha_5\beta_1$ (23), and in T-cells, where LFA-1-mediated cell binding was shown to be enhanced by clustering of membrane rafts *via* the GPI-anchored protein CD24 (24). In raft membranes, integrin-integrin contacts may be promoted by a more extreme hydrophobic environment, or by other physical properties such as membrane thickness (37). Raft localization could also regulate integrin clustering by its association with the actin cytoskeleton. In T cells, both raft localization and increased PKCθ association with the cytoskeleton was correlated with stimulation of IL-2 synthesis induced by CD47 ligation in synergy with TCR (10), suggesting that CD47 may link T cell signaling to the cytoskeleton through detergent-resistant domains. Although clustering of certain integrins can be enhanced with release of cytoskeletal constraints in lymphocytes (38), these linkages may also provide adhesive strength. Regulated distribution of transmembrane proteins to cytoskeletal-linked DRMs has been shown in mouse mammary epithelial cells, where CD44 partitioning was correlated with its redistribution to the leading edge of polarized cells (21). In a similar manner, CD47 may serve as a link between integrin surface clusters and the cytoskeleton. Interestingly, the cytoplasmic tail of CD47 has been found to associate with cytoplasmic proteins termed PLICs (proteins linking intermediate filaments to CD47), which may provide a link between CD47 containing complexes and the cytoskeleton (39). The ability of IgV-GPI to increase tethering of $\alpha_v\beta_3$ to the cytoskeleton (Fig. 7) indicates that the linkage need not be through CD47 itself, but that the IgV domain of CD47 confers upon the integrin an enhanced ability to engage cytoskeletal elements.

Recent structural studies of $\alpha_v\beta_3$ have provided new insights into how lateral or cis integrin ligands might inhibit or promote integrin activation. The crystal structure of $\alpha_v\beta_3$ reported by Xiong *et al.* (40, 41) showed the integrin in a bent conformation, and ultrastructural studies have depicted closed and open configurations that correlate with low and high affinity states, respectively (42). Thus regulation of integrin activation can be seen in terms of a conformational equilibrium that may be influenced in either direction by the action of ligands, antibodies or associated proteins. We have demonstrated in this study that CD47, though its extracellular IgV domain, can increase the appearance of LIBS epitopes that are exposed with RGD binding which leads to a more open conformation of the integrin (33). Thus in addition to effects on integrin clustering by recruitment to ordered lipid domains, CD47 may have direct conformational influences by stabilizing the open conformation of integrin heterodimers. However, IgV interaction alone was not sufficient for targeting integrin to cholesterol-rich rafts (Fig. 5*B*), indicating that CD47-$\alpha v\beta 3$ complexes in these domains may have different properties. Because the MMS region is strictly required for G protein association (Fig. 4*B*), localization to cholesterol-rich rafts may be an activating mechanism, with a requirement of integrin transmembrane contacts for G protein coupling (2). The finding that a CD47 extracellular epitope, detected by the mAb 10G2, is exposed with cholesterol depletion (9), indicates that membrane-proximal contacts influence IgV structure, and may therefore affect extracellular integrin contacts. Translocation of the CD47-$\alpha_v\beta_3$ complex between cholesterol-poor and cholesterol-rich domains could therefore alter the CD47 influence on integrin conformation, as well as activate G_i-mediated signaling. In support of such a

pathway, it has been reported that IGF-1 treatment of human SMC increased the affinity of $\alpha_v\beta_3$ for soluble vitronectin, and was accompanied by translocation of CD47 from Triton-insoluble to Triton-soluble fractions (20). Binding of 4N1K by the IgV domain could also produce signaling-dependent *versus* direct conformational outcomes. A recombinant cell-binding domain of thrombospondin has been shown to produce G_i-mediated effects requiring both VVM motifs from which the 4N1K sequence was derived, suggesting that G protein activation occurs via CD47 oligomerization (43). 4N1K-induced oligomerization of CD47 could lead to formation of higher order clusters through its association with integrin aggregates. While the process of G protein coupling by CD47 has not been fully elucidated, our findings that CD47-integrin complexes are altered by the lipid environment of the membrane may lead to new ways to approach the mechanism of signaling.

Our finding that CD47 can modulate $\alpha_v\beta_3$ avidity may resolve the apparently conflicting observations that CD47 exerts both signaling-dependent and signaling-independent effects on β_3 integrin function. Furthermore, we have shown that integrin recruitment to different membrane microdomains by CD47 can affect integrin activation by direct association, or by signaling through recruitment into cholesterol-rich rafts containing G_i. Thus different pools of $\alpha_v\beta_3$ can be regulated differently by CD47, perhaps leading to different biological readouts such as motility, protection from apoptosis or gene expression. The striking ability of different membrane environments to alter the interaction of CD47 with its integrin partner represents a unique example of how raft localization can modulate integrin functions, and may serve as a more general model for the interaction of other classes of integrin-associating proteins.

Acknowledgments—We thank Dr. Frederik Lindberg for preparation of the CD47 constructs and OV10 clones used in this study. We thank Dr. Mark Ginsberg for the LIBS antibodies and Dr. David Cheresh for the anti-$\alpha_v\beta_3$ and anti-$\alpha_v\beta_5$ antibodies. We also thank Dr. Linda Pike at the Washington University School of Medicine for assistance and equipment in detergent-free raft preparations.

REFERENCES

1. Brown, E. J. (2002) *Curr. Opin. Cell Biol.* **14,** 603–607
2. Brown, E. J., and Frazier, W. A. (2001) *Trends Cell Biol.* **11,** 130–135
3. Brown, E. J. (2001) *J. Clin. Investig.* **107,** 1499–1500
4. Gao, A. G., Lindberg, F. P., Dimitry, J. M., Brown, E. J., and Frazier, W. A. (1996) *J. Cell Biol.* **135,** 533–544
5. Wang, X. Q., and Frazier, W. A. (1998) *Mol. Biol. Cell* **9,** 865–874
6. Chung, J., Gao, A. G., and Frazier, W. A. (1997) *J. Biol. Chem.* **272,** 14740–14746
7. Chung, J., Wang, X. Q., Lindberg, F. P., and Frazier, W. A. (1999) *Blood* **94,** 642–648
8. Frazier, W. A., Gao, A. G., Dimitry, J., Chung, J., Brown, E. J., Lindberg, F. P., and Linder, M. E. (1999) *J. Biol. Chem.* **274,** 8554–8560
9. Green, J. M., Zheleznyak, A., Chung, J., Lindberg, F. P., Sarfati, M., Frazier, W. A., and Brown, E. J. (1999) *J. Cell Biol.* **146,** 673–682
10. Rebres, R. A., Green, J. M., Reinhold, M. I., Ticchioni, M., and Brown, E. J. (2001) *J. Biol. Chem.* **278,** 7672–7680
11. Manna, P. P., and Frazier, W. A. (2003) *J. Immunol.* **170,** 3544–3553
12. Fujimoto, T., Katsutani, S., Shimomura, T., and Fujimura, K. (2003) *J. Biol. Chem.* **278,** 26655–26665
13. Lindberg, F. P., Gresham, H. D., Reinhold, M. I., and Brown, E. J. (1996) *J. Cell Biol.* **134**, 1313–1322
14. Newman, P. J., Allen, R. W., Kahn, R. A., and Kunicki, T. J. (1985) *Blood* **65,** 227–232
15. Brown, E. J., and Goodwin, J. L. (1988) *J. Exp. Med.* **167,** 777–793
16. Lindberg, F. P., Gresham, H. D., Schwarz, E., and Brown, E. J. (1993) *J. Cell Biol.* **123,** 485–496
17. Kosfeld, M. D., and Frazier, W. A. (1992) *J. Biol. Chem.* **267,** 16230–16236
18. Weetall, M., Hugo, R., Friedman, C., Maida, S., West, S., Wattanasiu, S., Bouhel, R., Weitz-Schmidt, G., and Lake, P. (2001) *Anal. Biochem.* **293,** 277–287
19. Smart, E. J., Ying, Y. S., Mineo, C., and Anderson, R. G. W. (1995) *Proc. Natl. Acad. Sci. U. S. A.* **92,** 10104–10108
20. Maile, L. A., Inai, Y., Clarke, J. B., and Clemmons, D. R. (2002) *J. Biol. Chem.* **277,** 1800–1805
21. Oliferenko, S., Paika, K., Harder, T., Gerke, V., Schwarzler, C., Schwarz, H., Beug, H., Gunthert, V., and Huber, L. A. (1999) *J. Cell Biol.* **146,** 843–854
22. Rebres, R. A., Vaz, L. E., Green, J. M., and Brown, E. J. (2001) *J. Biol. Chem.* **276,** 2001
23. Gopalakrishna, P., Chaubey, S. K., Manogaran, P. S., and Pande, G. (2000) *J. Cell. Biochem.* **77,** 517–528
24. Marwali, M. R., Rey-Ladino, J., Dreolini, L., Shaw, D., and Takei, F. (2003) *Blood* **102,** 215–222
25. Barazi, H., Li, Z., cashel, J. A., Krutzsch, H. C., Annis, D. S., Mosher, D. F., and Roberts, D. D. (2002) *J. Biol. Chem.* **277,** 42859–42866
26. Tulasne, D., Judd, B. A., Johansen, M., Asazuma, N., Best, D., Brown, E. J., Kahn, M., Koretzky, G. A., and Watson, S. P. (2001) *Blood* **98,** 3346–3352
27. Brown, D. A., and London, E. (2000) *J. Biol. Chem.* **275,** 17221–17224
28. Pike, L. J., Han, X., Chung, K. N., and Gross, R. W. (2002) *Biochemistry* **41,** 2075–2078
29. Pierini, L. M., and Maxfield, F. R. (2001) *Proc. Natl. Acad. Sci. U. S. A.* **98,** 9471–9473
30. Kasahara, K., Watanabe, K., Takeuchi, K., Kaneko, H., Oohira, A., Yamamoto, T., and Sanai, Y. (2000) *J. Biol. Chem.* **275,** 34701–34709
31. Braccia, A., Villam, M., Immerdal, L., Niels-Christianson, L. L., Nystrom, B. T., Hansen, G. H., and Danielson, E. M. (2003) *J. Biol. Chem.* **278,** 15679–15684
32. Schuck, S., Housho, M., Ekros, K., Shevchenko, A., and Simons, K. (2003) *Proc. Natl. Acad. Sci. U. S. A.* **100,** 5795–5800
33. Hynes, R. O. (2002) *Cell* **110,** 673–687
34. Wang, X. Q., Lindberg, F. P., and Frazier, W. A. (1999) *J. Cell Biol.* **147,** 389–400
35. Li, R., Mitra, N., Gratkowski, H., Vilaire, G., Litvinov, R., Nagasami, C., Weisel, J. W., Lear, J. D., Delgrado, W. F., and Bennett, J. S. (2003) *Science* **300,** 795–798
36. Vinogradova, O., Velyvis, A., Velyviene, A., Hu, B., Haas, T. A., Plow, E. F., and Qin, J. (2002) *Cell* **110,** 587–597
37. Reitvold, A., and Simons, K. (1998) *Biochim. Biophys. Acta* **1376,** 467–479
38. Lub, M., Kooyk, Y. v., Vliet, S. J., and Figdor, C. G. (1997) *Mol. Biol. Cell* **8,** 341–351
39. Wu, A. L., Wang, J., Zheleznyak, A., and Brown, E. J. (1999) *Mol. Cell* **4,** 619–625
40. Xiong, J. P., Stehle, T., Dietenbach, B., Zhang, R., Dunker, R., Scott, D. L., Joachimiak, A., Goodman, S. L., and Arnaoult, M. A. (2001) *Science* **294,** 339–345
41. Xiong, J. P., Stehle, T., Zhang, R., Joachimiak, A., Frech, M., Goodman, S. L., and Arnaoult, M. A. (2002) *Science* **296,** 151–155
42. Tagaki, J., Petre, P. M., Walz, T., and Springer, T. A. (2002) *Cell* **110,** 599–603
43. McDonald, J. F., Dimitry, J. D., and Frazier, W. A. (2003) *Biochemistry* **42,** 10001–10011